Neuron, Volume *59*

Supplemental Data

Coordinated Actions of the Forkhead Protein Foxp1 and Hox Proteins in the Columnar Organization of Spinal Motor Neurons

David L. Rousso, Zachary B. Gaber, Deneen Wellik, Edward E. Morrisey, and Bennett G. Novitch

Supplemental Experimental Procedures

Antibodies

Antibodies against a conserved peptide in the c-terminal end of chick Foxp1 (DFDHDRDYEDEPVNEDIE) were raised in guinea pigs. Additional antibodies used include: rabbit anti-Foxp1 (Abcam, Ab16645); goat anti-Isl1 (R&D Systems); rabbit anti-Isl1/2 (K5), rabbit anti-Isl1 (A8), guinea pig anti-Isl1, mouse anti-Isl1/2 (4D5), rabbit anti-Lhx3, mouse anti-Lhx3 (4E12), rabbit anti-Lhx1, mouse anti-Lhx1 (4F2), rabbit anti-Nkx6.1, rabbit anti-Raldh2, rabbit anti-Hb9, mouse anti-Mnr2/Hb9 (5C10), mouse anti-neurofilament (2H3) (Kania et al., 2000; Novitch et al., 2001; Novitch et al., 2003 and references therein); guinea pig anti-Lhx3, guinea pig anti-Hb9 (Thaler et al., 2004); rabbit anti-EphA4 (SC-921), goat anti-Hoxc6 (Santa Cruz, SC-46135); mouse anti-Hoxc8 (Covance); guinea pig anti-Hoxa5, rabbit anti-Hoxc9, rabbit anti-Hoxa10 (Dasen et al., 2005); rabbit anti-Pea3 (Arber et al., 2000); rabbit anti-Er81 (Covance); Rabbit anti-Runx1 (Sigma); Rabbit anti-SCIP (Ilia et al., 2002); guinea pig anti-Raldh2 (Ji et al., 2006); sheep anti-GFP (Biogenesis); rabbit anti-GFP (Invitrogen); rabbit anti-nNOS (Immunostar), rabbit anti-VAChT (Chemicon); mouse anti-NAPA-73 (E/C8; Yip et al., 1998); Rabbit anti-HRP (Jackson Immunoresearch). Alexa488-, FITC-, Cy3- and Cy5-conjugated secondary antibodies were obtained from either Invitrogen or Jackson Immunoresearch.

In Situ Probes

The in situ probe against the 3' coding region and UTR of the chick *Foxp1* mRNA was prepared using the following primers: forward, 5'-AAGGGGCAGTATGGACAGTG-3'; reverse, 5'-GAGATTAACCCTCACTAAAGGGAACAAGTCCATCCAATGCACA-3'. Underlined portion indicates a T3 RNA polymerase site embedded in the primer sequence.

In Ovo Electroporation

HH stage 12-14 chick embryos were electroporated as previously described (Novitch et al., 2001; Novitch et al., 2003), and incubated for ~72 hours to HH stages 25-27 before collection and fixation. Expression vectors for Foxp1 and Lhx3 were generated by subcloning the mouse Foxp1A and chick Lhx3 genes into the pCIG expression vector (Megason and McMahon, 2002).

Supplemental References

Arber, S., Ladle, D. R., Lin, J. H., Frank, E., and Jessell, T. M. (2000). ETS gene Er81 controls the formation of functional connections between group Ia sensory afferents and motor neurons. Cell 101, 485-498.

Dasen, J. S., Tice, B. C., Brenner-Morton, S., and Jessell, T. M. (2005). A Hox regulatory network establishes motor neuron pool identity and target-muscle connectivity. Cell 123, 477-491.

Ilia, M., Beasley, C., Meijer, D., Kerwin, R., Cotter, D., Everall, I., and Price, J. (2002). Expression of Oct-6, a POU III domain transcription factor, in schizophrenia. Am J Psychiatry 159, 1174-1182.

Ji, S. J., Zhuang, B., Falco, C., Schneider, A., Schuster-Gossler, K., Gossler, A., and Sockanathan, S. (2006). Mesodermal and neuronal retinoids regulate the induction and maintenance of limb innervating spinal motor neurons. Dev Biol 297, 249-261.

Kania, A., Johnson, R. L., and Jessell, T. M. (2000). Coordinate roles for LIM homeobox genes in directing the dorsoventral trajectory of motor axons in the vertebrate limb. Cell 102, 161-173.

Megason, S. G., and McMahon, A. P. (2002). A mitogen gradient of dorsal midline Wnts organizes growth in the CNS. Development 129, 2087-2098.

Novitch, B. G., Chen, A. I., and Jessell, T. M. (2001). Coordinate regulation of motor neuron subtype identity and pan-neuronal properties by the bHLH repressor Olig2. Neuron 31, 773-789.

Novitch, B. G., Wichterle, H., Jessell, T. M., and Sockanathan, S. (2003). A requirement for retinoic acid-mediated transcriptional activation in ventral neural patterning and motor neuron specification. Neuron 40, 81-95.

Thaler, J. P., Koo, S. J., Kania, A., Lettieri, K., Andrews, S., Cox, C., Jessell, T. M., and Pfaff, S. L. (2004). A postmitotic role for Isl-class LIM homeodomain proteins in the assignment of visceral spinal motor neuron identity. Neuron 41, 337-350.

Yip, J. W., Yip, Y. P., and Capriotti, C. (1998). Segmental specificity of chick sympathetic preganglionic projections is influenced by preganglionic neurons from neighboring spinal cord segments. J Neurosci 18, 10473-10480.

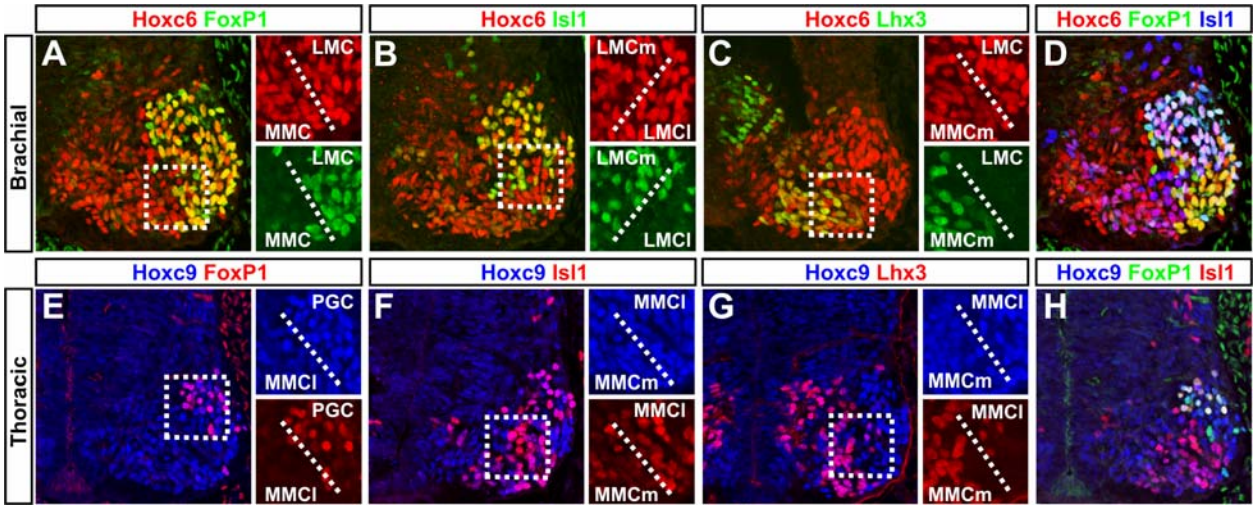

Figure S1. Hoxc6 and Hoxc9 Are Expressed by Multiple Motor Columns in the Brachial and Thoracic Spinal Cord

(A-D) At brachial levels, Hoxc6 protein expression can be observed in $Foxp1^{+}$ $Isl1^{+}$ LMCm MNs, $Foxp1^{+}$ $Isl1^{-}$ LMCl MNs, and $Lhx3^{+}$ $Isl1^{+}$ MMCm MNs.

(E-H) At thoracic levels, Hoxc9 expression can be observed in $Foxp1^{+}$ $Isl1^{+}$ PGC MNs, $Foxp1^{-}$ $Isl1^{+}$ MMCl MNs, and $Lhx3^{+}$ $Isl1^{+}$ MMCm MNs.

See Table 1, Figure 1, and the text for details on the use of Foxp1 as a marker of LMC and PGC MNs.

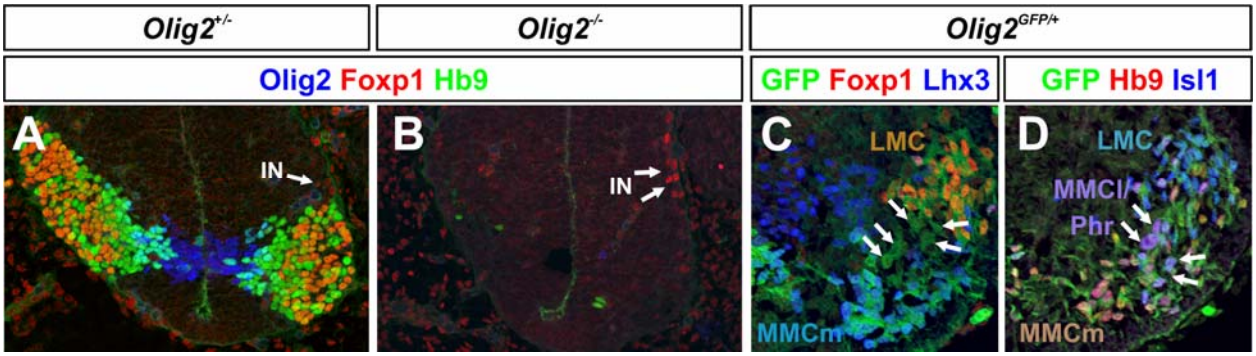

Figure S2. Foxp1 Is Expressed by a Subset of Olig2-Derived MNs and Lost in Olig2 Mutants
(A-B) Analysis of Foxp1 and Hb9 in e10.5 control and Olig2 mutant spinal cords. Note that in addition to MNs, Foxp1 is expressed by a small number of ventral interneurons (IN). These Foxp1^{+} interneurons appear to be slightly increased in the Olig2 mutants.
(C-D) Short-term lineage tracing of Olig2-derived cells using GFP expressed in e11.5 Olig2$^{GFP/+}$ knock-in mice. Arrows indicate Olig2-derived MMCl cells that lack expression of both Foxp1 and Lhx3, but express high levels of Hb9 and Isl1.

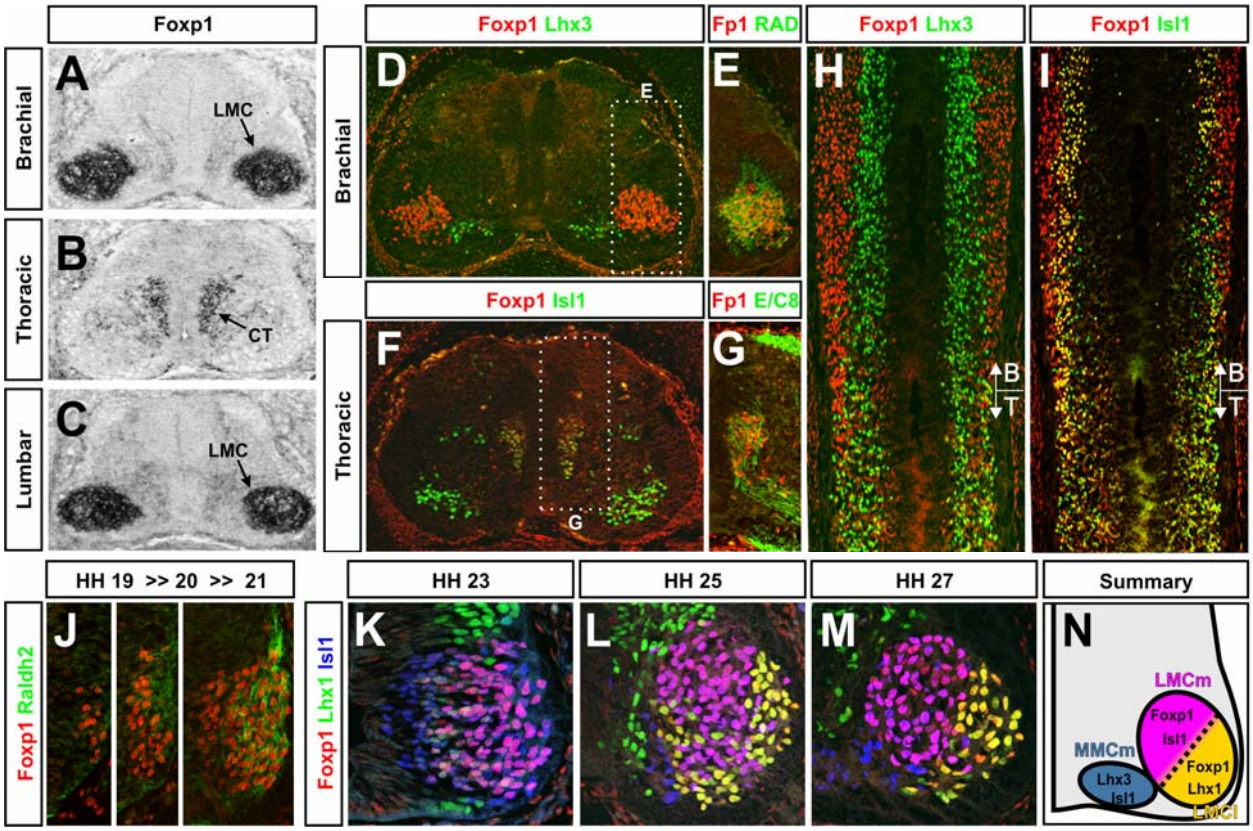

Figure S3. Analysis of Foxp1 Expression in the Chick Spinal Cord

(A-C) Analysis of *Foxp1* mRNA expression in the HH stage 29 chick spinal cord at brachial, thoracic, and lumbar levels.

(D-G) Antibody costaining analysis of stage 29 brachial and thoracic spinal cord sections.

(H-I) Longitudinal staining of Foxp1, Lhx3, and Isl1 at the brachial-thoracic (B-T) junction.

(J) Comparison of the onset of Foxp1 and Raldh2 in the brachial spinal cord at HH stages 19, 20, and 21.

(K-M) Emergence and lateral migration of $Lhx1^{+}$ LMCl MNs from $Foxp1^{+}$ cells.

(N) Summary of the distribution of Foxp1 in forelimb level motor columns.

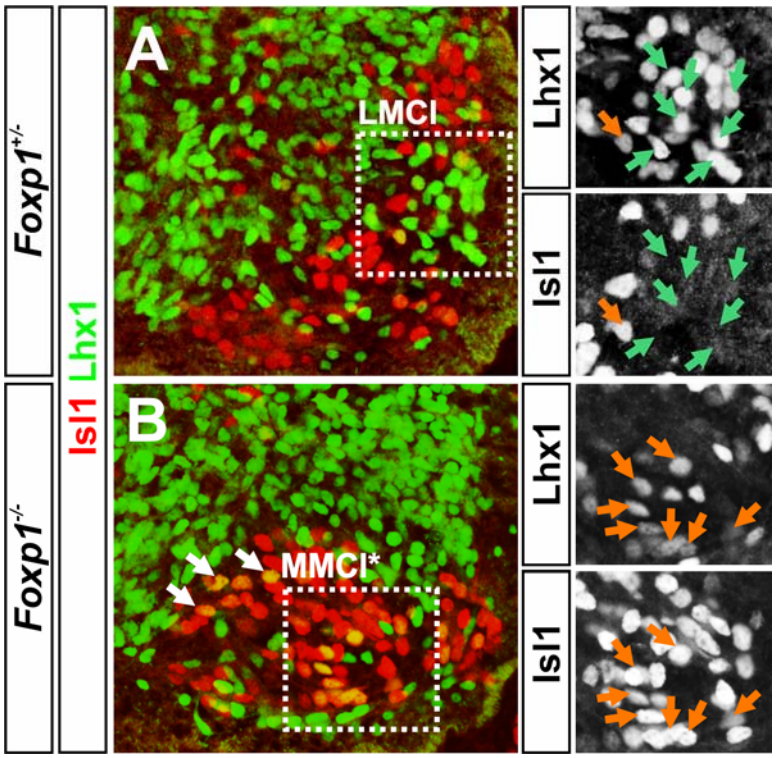

Figure S4. Aberrant Coexpression of Lhx1 and Isl1 in Foxp1 Mutant MNs

(A-B) Antibody costaining analysis of MNs in *Foxp1*$^{+/-}$ control and *Foxp1*$^{-/-}$ mutant spinal cords. Whereas Lhx1 and Isl1 expression is normally mutually exclusive in LMCl and LMCm MNs, respectively, numerous Lhx1^{+} Isl1^{+} cells can be seen in the MMCl-like MNs that form in the Foxp1 mutants.

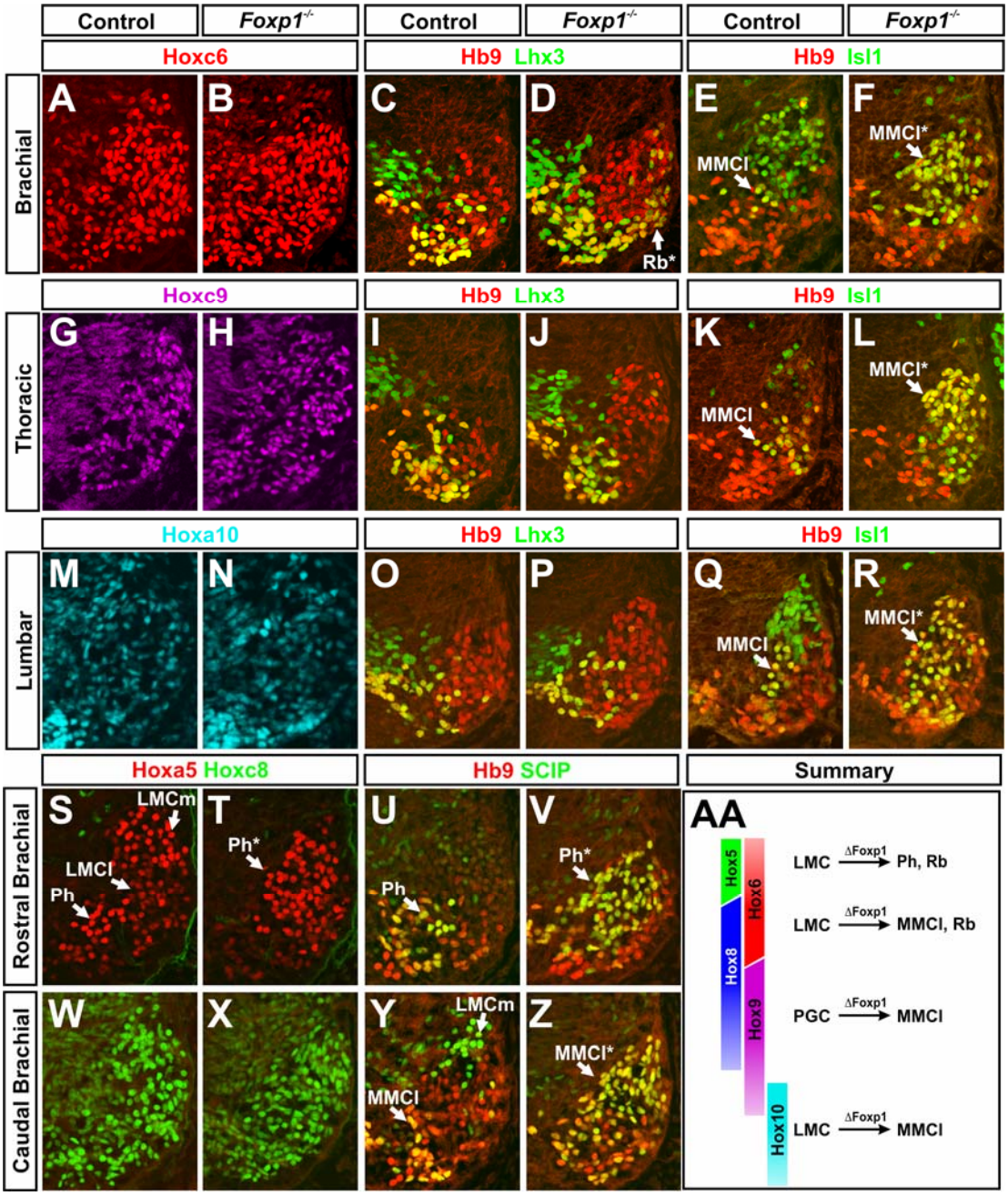

Figure S5. Correspondence of the Phenotypes in the Foxp1 Mutants with the Intact Pattern of Hox Protein Expression

(A, B, G, H, M, N, S, T, W, X) At brachial, thoracic, and lumbar levels, the expression of Hoxa5, Hoxc6, Hoxc8, Hoxc9, and Hoxa10 does not appear to be changed in the Foxp1 mutants.

(C, D, I, J, O, P) The appearance of ectopic laterally positioned Lhx3^{+} MNs in the Foxp1 mutants only occurs in the brachial spinal cord where Hoxc6 is expressed. Rb*, rhomboideus-like MNs.

(E, F, K, L, Q, R) In contrast, the formation of ectopic Hb9^{+} Isl1^{high} MMCl-like MNs (MMCl*) occurs at each axial level of the Foxp1 mutant spinal cord.

(S-Z) Ectopic Hb9^{+} SCIP^{high} MMCl-like MNs that form in the rostral and caudal portions of the forelimb maintain their appropriate segmental expression of Hoxa5 and Hoxc8, subdividing the MMCl into territories that produce phrenic MNs (Ph) vs. other MMCl MN populations.

(AA) Summary indicating that at each level of the spinal cord, the loss of Foxp1 leads to a transformation of LMC and PGC MNs towards MMC MN fates that are associated with specific Hox protein expression profiles.

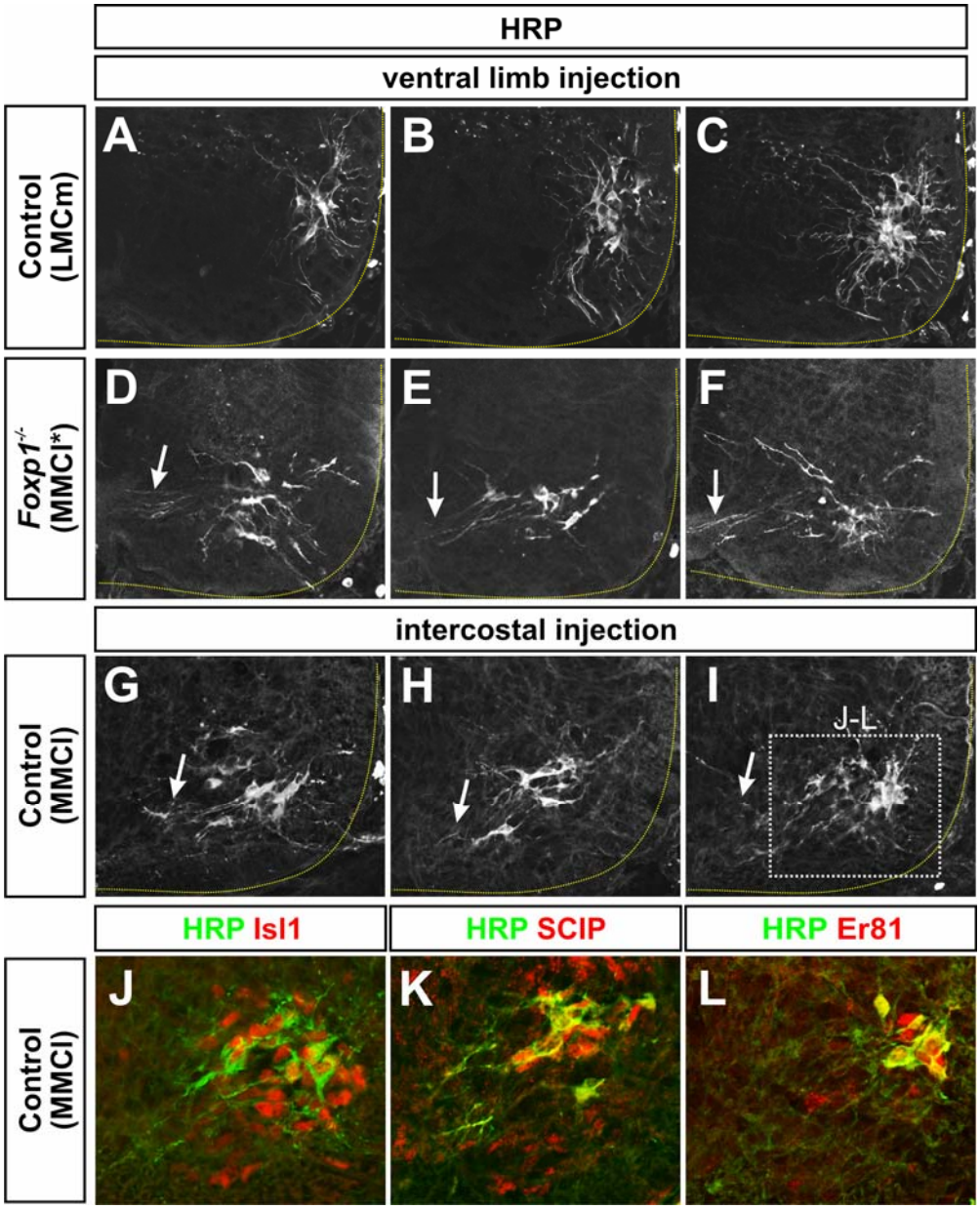

Figure S6. Foxp1 Mutant MNs that Project to the Ventral Forelimb Muscles Display a MMCl-like Settling Position and Dendritic Morphology

(A-F) Representative images of MNs labeled by HRP injections into ventral forelimb muscles of e13.0-e13.5 control and Foxp1 mutant mice.

(G-I) Similar labeling of MNs by HRP injections into intercostal muscles in control embryos.

In control spinal cords, ventral forelimb muscle injections label cells clustered in a dorsolateral position and displaying a radial dendritic morphology. In contrast, similarly labeled MNs in the Foxp1 mutants are clustered in a more ventromedial position that coincides with the settling position of MMCl MNs. In addition, the Foxp1 mutant MN dendrites have a different appearance with long lateral processes that extend towards the midline (arrows in D-F), again similar to MMCl MNs (arrows in G-I).

(J-L) HRP labeled intercostal MNs express the MMCl-T markers Isl1, SCIP, and Er81.

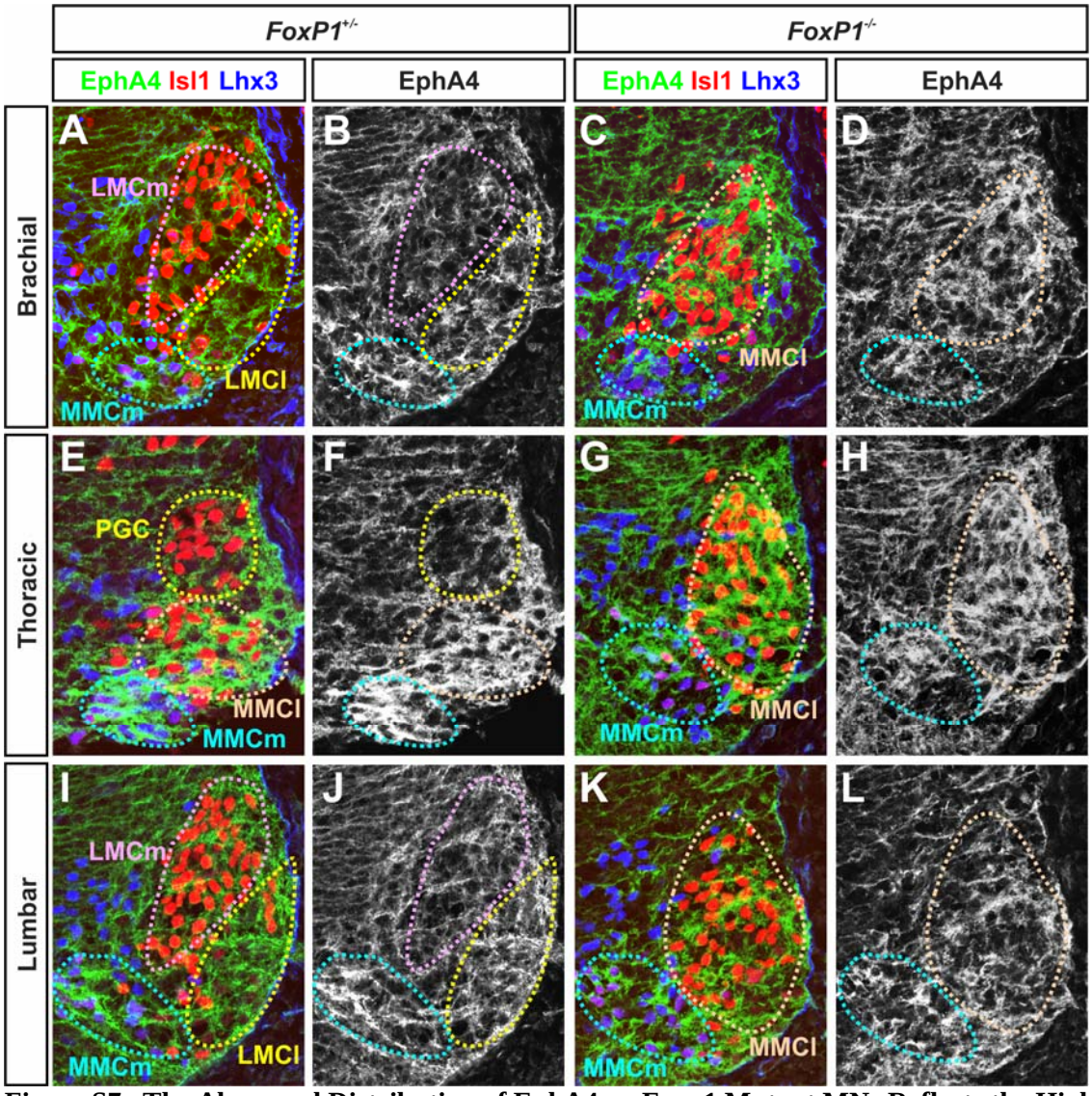

Figure S7. The Abnormal Distribution of EphA4 on Foxp1 Mutant MNs Reflects the High Levels of EphA4 Expression Normally Associated with MMCl MNs

(A-L) Costaining analysis of the ventrolateral quadrant of control and Foxp1 mutant spinal cords using the indicated antibodies. Location of different populations of MNs were determined based on their LIM-HD expression profile and used to display where different levels of EphA4 expression can be detected.

(A, B, E, F, I, and J) In control spinal cords, EphA4 protein appears to be selectively reduced on LMCm and PGC MNs. Note that EphA4 is highly expressed in the $Lhx3^{-}$ $Isl1^{+}$ MMCl MNs seen at thoracic levels

(C, D, G, H, K, L) In Foxp1 mutants, EphA4 expression is high in most MN populations, particularly the expanded MMCl MNs.